| REPORT DOCUMENTATION PAGE | | Form Approved OMB No. 0704-0188 |
|---|---|---|

Public reporting burden for this collection of information is estimated to average 1 hour per response, including the time for reviewing instructions, searching existing data sources, gathering and maintaining the data needed, and completing and reviewing this collection of information. Send comments regarding this burden estimate or any other aspect of this collection of information, including suggestions for reducing this burden to Department of Defense, Washington Headquarters Services, Directorate for Information Operations and Reports (0704-0188), 1215 Jefferson Davis Highway, Suite 1204, Arlington, VA 22202-4302. Respondents should be aware that notwithstanding any other provision of law, no person shall be subject to any penalty for failing to comply with a collection of information if it does not display a currently valid OMB control number. **PLEASE DO NOT RETURN YOUR FORM TO THE ABOVE ADDRESS.**

| 1. REPORT DATE (DD-MM-YYYY) 02-28-2007 | 2. REPORT TYPE Final | 3. DATES COVERED (From - To) 2-1-2006 to 11-30-2006 |
|---|---|---|

**4. TITLE AND SUBTITLE**

Stabilization and Carbonization of Gel Spun Polyacrylonitrile/Single Wall Carbon Nanotube Composite

Fibers

**5a. CONTRACT NUMBER**
FA9550-06-1-0122

**5b. GRANT NUMBER**

**5c. PROGRAM ELEMENT NUMBER**

**6. AUTHOR(S)**

Satish Kumar, Han Gi Chae, Marilyn Minus, Asif Rasheed

**5d. PROJECT NUMBER**

**5e. TASK NUMBER**

**5f. WORK UNIT NUMBER**

**7. PERFORMING ORGANIZATION NAME(S) AND ADDRESS(ES)**
School of Polymer, Textile and Fiber Engineering
Georgia Institute of
Technology
Atlanta GA 30332-0295

**8. PERFORMING ORGANIZATION REPORT NUMBER**

**9. SPONSORING / MONITORING AGENCY NAME(S) AND ADDRESS(ES)**
AFOSR/NL
875 Randolph St
Arlington VA 22203-1954

Dr Charles Lee

**10. SPONSOR/MONITOR'S ACRONYM(S)**

**11. SPONSOR/MONITOR'S REPORT NUMBER(S)**

**12. DISTRIBUTION / AVAILABILITY STATEMENT**

Approved for public release,
distribution unlimited

AFRL-SR-AR-TR-07-0088

**13. SUPPLEMENTARY NOTES**

**14. ABSTRACT**
Gel spun polyacrylonitrile (PAN) and PAN/single wall carbon nanotube (SWNT) composite fibers have been stabilized in air and subsequently carbonized in argon at 1100 °C. Differential scanning calorimetry (DSC) and infrared spectroscopy suggests that the presence of single wall carbon nanotube affects PAN stabilization. Carbonized PAN/SWNT fibers exhibited 10 to 30 nm diameter fibrils embedded in brittle carbon matrix, while the control PAN carbonized under the same conditions exhibited brittle fracture with no fibrils. High resolution transmission electron microscopy and Raman spectroscopy suggests the existence of well developed graphitic regions in carbonized PAN/SWNT and mostly disordered carbon in carbonized PAN. Tensile modulus and strength of the carbonized fibers were as high as 250 N/tex and 1.8 N/tex for the composite fibers and 168 N/tex and 1.1 N/tex for the control PAN based carbon fibers, respectively. The addition of 1 wt% carbon nanotubes enhanced the carbon fiber modulus by 49% and strength by 64%.

# 20070417174

**15. SUBJECT TERMS**

| 16. SECURITY CLASSIFICATION OF: | | | 17. LIMITATION OF ABSTRACT | 18. NUMBER OF PAGES | 19a. NAME OF RESPONSIBLE PERSON |
|---|---|---|---|---|---|
| a. REPORT | b. ABSTRACT | c. THIS PAGE | | | 19b. TELEPHONE NUMBER (include area code) |

Standard Form 298 (Rev. 8-98)
Prescribed by ANSI Std. Z39.18

## Introduction

Polyacrylonitrile (PAN) is currently the predominant precursor for carbon fibers[1-6]. Carbon nanotubes (CNT) can be well dispersed in PAN resulting in PAN/CNT composite fiber modulus consistent with theoretical predictions[7, 8] or higher[9]. High orientation of exfoliated single wall carbon nanotubes (SWNTs) can be obtained in PAN via gel spinning[9]. Stabilization and carbonization of PAN/vapor grown carbon nanofiber (VGCNF) and PAN/multiwall nanotube (MWNT) composite films processed by gel drawing, resulted in carbon films with a modulus of about 30 GPa[10-12]. It has also been reported that oxidatively stabilized PAN/SWNT fibers containing 10 wt% SWNT exhibit significantly higher tensile strength and modulus than the PAN fiber stabilized under the same conditions[13]. Highly drawn gel spun fiber containing 1 wt% SWNT were processed where nanotubes were mostly individuals rather than bundles[9]. Highly drawn gel spun PAN fibers could be dissolved when boiled in dimethylformamide (DMF). On the other hand, highly drawn gel spun PAN/SWNT fibers containing 1 wt% SWNT, when boiled in DMF results in fibrillar dispersion. Examination of these fibrils in the high resolution transmission electron microscope showed that these fibrils are composed of mostly well separated SWNTs covered with PAN and the typical diameter of these fibrils is in the range of 10 to 30 nm (Figure 1). In this paper, stabilization and carbonization studies on highly drawn gel spun PAN/SWNT composite fibers containing 0.5 and 1 wt% SWNT are reported.

## Experimental

PAN and PAN/SWNT composite fibers were processed by gel spinning as described elsewhere[9]. PAN was supplied by Exlan, Co. (Japan) and the viscosity average molecular weight was 250,000 g/mol. SWNTs (lot number XO1PPP) were obtained from Carbon Nanotechnologies, Inc. (Houston, TX) and the catalytic impurity was determined to be about 1 wt% by thermogravimetric analysis (TGA). At 1 wt% SWNT in PAN, this represents an impurity level of 0.01 wt% in the PAN/SWNT precursor fiber. Fibers were processed using spinnerets of 500 and 250 µm diameters. All PAN and PAN/SWNT fibers in this study were drawn to a draw ratio of 38. Differential scanning calorimetry (DSC) on the precursor fibers was conducted by heating from 40 to 400 $^o$C at a heating rate of 1 $^o$C/min. After the 1$^{st}$ heating scan, the sample pan in the DSC furnace was quenched to 40 $^o$C at a rate of 100 $^o$C/min. This heating/cooling cycle was repeated two more times.

For stabilization, fibers were clamped between two carbon steel blocks and hung over a quartz rod (Figure 2), and stabilization was carried out in a box furnace (Lindberg, 51668-HR Box Furnace 1200C, Blue M Electric) in air at various stress levels (0.025, 0.017, 0.009 and 0.006 N/tex, stress is based on the linear density of the precursor fiber). Fibers were heated from room temperature to 285 $^o$C in air at a heating rate of 1 $^o$C/min and held at 285 $^o$C for 10 hr followed by heating up to 330 $^o$C at a heating rate of 1 $^o$C/min and held at 330 ºC for 3 hr (Figure 3a). The stabilized fibers were cooled down to room temperature over a period of several hours. The stabilized PAN and PAN/SWNT fibers were subsequently carbonized in argon by heating from room temperature at a rate of 5 $^o$C/min, and by holding at 1100 $^o$C for 5 minutes at various stress levels (0.025, 0.017, 0.009 and 0.006 N/tex, stress is based on the linear density of the precursor fiber). In the initial study, the precursor fiber diameter was 20 to 23 µm, resulting in 12 to 13 µm diameter carbon fibers (also referred to as large diameter fibers). Since higher tensile strength can be obtained in smaller diameter fibers, PAN and PAN/SWNT (99/1) fibers were also gel spun with a diameter of about 12 µm (with a draw ratio of 38). These fibers resulted in about 6 µm diameter carbon fibers (also referred to as small diameter fibers). The stabilization and carbonization heating profiles for the small diameter fibers are shown in Figure 3b. As can be seen in Figure 3b, shorter stabilization time was used for the smaller diameter fibers, while the carbonization time and temperature for both types of fibers were the same.

Infra-red spectroscopy was conducted on the stabilized fibers using Perkin Elmer FT-IR microscope and by collecting 2048 scans at a resolution of 4 cm$^{-1}$. The PeakFit (v4.11) was used to analyze conjugated ($\sim$2210 cm$^{-1}$) and β-amino ($\sim$2190 cm$^{-1}$) nitrile groups[14-19], as well as the unreacted nitrile band at $\sim$2240 cm$^{-1}$. Raman spectra of precursor and carbonized fibers were collected in the back scattering geometry using Holoprobe Research 785 Raman Microscope made by Kaiser Optical System using 785 nm excitation laser with polarizer and analyzer parallel to each other (vv mode), and the fibers were placed parallel to the polarizer and analyzer. Wide angle X-ray diffraction (WAXD) patterns were obtained on multifilament bundles on Rigaku Micromax-002 (X-ray wavelength, λ = 0.15418 nm) using Rigaku R-axis IV++ detection system. The diffraction patterns were analyzed using AreaMax V. 1.00 and MDI Jade 6.1. Crystallinity was determined by de-convoluting the integrated WAXD patterns and by using the ratio of the area of the crystalline peaks to the total area. Orientation (fc) of the PAN, as well as stabilized and carbonized fibers was determined using the azimuthal scans at two theta of 17, 26, and 26 degrees, respectively in conjunction with the Wilchinsky's equation[20]. Crystallite sizes (L) were determined from the WAXD data using the Scherrer equation with K=0.9[21]. Fiber tensile fracture surfaces were observed on the gold coated samples by scanning electron microscopy (LEO 1530 SEM operated at 10 kV). High resolution transmission electron microscopy (HRTEM) study was conducted using Hitachi HF-2000 (operated at 200 kV). For TEM specimen preparation, the carbonized fibers were ground using pestle and mortar into very fine powder. The ground powder was collected on lacey carbon coated copper grids. In HRTEM, beam alignment and stigmation corrections were first performed using evaporated aluminum standard on TEM grid (catalog number 80044, EMS, Co., Hatfield, PA) before inserting the actual sample. Single filament tensile properties were determined using RSA III solids analyzer (Rheometric Scientific, Co.) at a gauge length of 25 mm and the crosshead speed of 0.25 mm/s. For each

## Results and Discussion

Tensile properties and structural parameters of gel spun PAN and PAN/SWNT (99/1) fibers are listed in Table 1. PAN/SWNT precursor fibers exhibit moderately higher crystal orientation and crystallinity and smaller crystal size than the control PAN fiber. SWNT orientation ($f$SWNT) in composite fiber was determined to be 0.904 using the Raman G-band[9].

DSC thermograms of PAN and PAN/SWNT fibers under air show that the heat evolved in the composite fibers during stabilization is less than that in the control fiber (Figure 4 and Table 2). This suggests that the presence of SWNT hinders PAN stabilization reaction. As a result, we decided to use a relatively long stabilization time (Figure 3). SWNTs have good interaction with PAN[7-10, 13, 22-27]. As a result, PAN in the vicinity of SWNT becomes insoluble in DMF. The DSC study suggests that, as a result of PAN-SWNT interaction, PAN in the vicinity of SWNT has higher thermal stability than PAN without SWNT. This explains the reduced heat of stabilization for PAN/SWNT fiber as compared to the control PAN. PAN shows no heat evolution during the third heating cycle, while PAN/SWNT (99/1) fibers still shows about 30 J/g of heat of stabilization reaction. This suggests that stabilization in PAN/SWNT is still continuing, while stabilization in PAN was not observable (by DSC) during the third heating cycle.

Infra-red spectra of fibers stabilized with and without stress are shown in Figure 5. Stabilization without stress was carried out in air in a thermogravimetric analyzer (TGA) for 30 min. The chemical structures of various nitrile groups are shown in Figure 6. The conjugated nitrile group can be generated upon dehydrogenation of PAN and β-amino nitrile groups[28] can be formed due to the termination of cyclization reaction. The termination of cyclization is thought to take place every 4 – 5 PAN repeat units, a result of its helical conformation[19, 29]. Therefore, more planar zigzag conformation in the fiber is expected to increase the gap between cyclization termination. Chain scission may occur during cyclization termination. Therefore, the fiber containing more planar zigzag conformations would result in less frequent chain scission, and hence result in less defects, thus ultimately affecting the tensile strength of the resulting carbon fiber. The PAN/SWNT gel fiber has more planar zigzag sequences than the PAN fiber[9]. This difference may affect stabilization. Since the peak positions of different types of nitrile groups are known, the nitrile spectra was fitted without varying the peak position, and by allowing the peak width and intensity to vary (Figure 7), and the data is compared in Table 3. There are more unreacted nitrile groups in PAN/SWNT stabilized under stress than in the control PAN stabilized under the same conditions, and the quantity of unreacted groups increased with increasing stress as judged by the relative areas of the FTIR peaks. This confirms that the presence of SWNT as well as stress hinders stabilization reaction. PAN/SWNT samples stabilized in furnace under stress, exhibited significantly higher conjugated nitrile and significantly lower β-amino nitrile than the control PAN stabilized under the same conditions. The stabilized structure in PAN/SWNT predominantly contains conjugated nitrile, while in PAN it is predominantly βamino nitrile. This further suggests that SWNTs constrains PAN molecules and hence results in the higher degree of cyclization as discussed earlier. When stabilized in TGA, both PAN and PAN/SWNT fibers have very comparable amounts of different nitrile groups after 30 minutes of heat-treatment in air at 285 ºC. We think that during this short stabilization time, core of the fiber is mostly un-stabilized and hence the effect of the presence of SWNTs is not that obvious.

PAN molecules in the interphase region have higher orientation than in the matrix[9]. PAN/SWNT composite fibers show fibrillar structure even after stabilization and carbonization (Figure 8). The carbonized composite fiber contains nanofibrils embedded in the brittle carbon matrix. Nanofibrils consists of SWNTs surrounded by well developed graphitic structure (Figure 9a-f). PAN molecules in the interphase region when carbonized form well ordered graphite, while PAN matrix at this carbonization temperature is mostly disordered or amorphous carbon (Figure 9g).

The Raman spectra of carbonized PAN fibers show strong disorder band (at ~ 1300 cm$^{-1}$) and begins to show a shoulder for the graphitic G-band (at ~1580 cm$^{-1}$) when stress is increased during stabilization and carbonization (Figure 10A). On the other hand, carbonized PAN/SWNT fiber exhibits a distinct G band even when stabilized and carbonized at a low stress (Figure 10B). The G band intensity increases with increasing stress, confirming stress induced graphitization. The Raman observation is in agreement with high resolution transmission electron microscopy, showing less ordered carbon for carbonized PAN and well ordered carbon for carbonized PAN/SWNT. It should also be noted that the G band in carbonized PAN/SWNT fibers in Figure 10B is not due SWNTs. Due to resonance, SWNTs result in a very stromng intensity G band as can be seen in the PAN/SWNT precursor fiber (Figure 11). In the stabilized and carbonized fiber laser is absorbed by the stabilized and carbonized products of PAN, quenching SWNT spectra.

PAN based fibers are typically carbonized in the 1300 to 1700 ºC and result in disordered carbon. In order to develop graphitic structure, PAN based fibers are typically carbonized in the 2500 to 3000 ºC. Development of graphitic structure (as evidenced by Raman G band and high resolution transmission electron microscopy) in PAN/SWNT at a relatively low carbonization temperature of 1100 ºC suggests that the presence of SWNT not only affects PAN stabilization, but also leads to more graphitic structure at a relatively low carbonization temperature. Therefore PAN/SWNT (or perhaps PAN/carbon nanotubes) may represent a precursor for next generation carbon fiber with significantly higher modulus and strength than the current state of the art PAN based carbon fibers.

Figure 12 shows WAXD patterns and integrated scans for the precursor, stabilized, and carbonized fibers.

Higher orientation and larger crystal size were observed for the stabilized and carbonized PAN/SWNT fibers than that for the respective control fibers (Tables 4 and 5). Orientation and crystal size also increased with increasing applied stress during stabilization and carbonization. The structural parameters of pitch (P25) and PAN based (T300 and IM8) commercial carbon fibers are also listed in Table 5 for comparison.

Tensile modulus of the stabilized PAN/SWNT fibers is about 26% higher than the stabilized PAN fibers while the tensile strength and strain to failure of the two fibers were quite comparable (Table 6). Increased stress during stabilization resulted in higher modulus and tensile strength. Fiber shrinkage decreases with increasing applied stress during stabilization (Figure 13). Also at a given stress, less shrinkage is observed in PAN/SWNT than in PAN. The shrinkage data is based on the fiber length measurement before and after stabilization.

Carbonized PAN/SWNT fiber exhibit higher tensile strength and modulus than the control PAN fiber processed under the same conditions (Table 7). The addition of 1 wt% SWNT resulted in 64% increase in tensile strength and 49% increase in modulus for the small diameter carbon fiber. The substantially higher modulus in carbonized PAN/SWNT as compared to carbonized PAN is attributed to higher orientation and higher graphitic order. On the other hand tensile strength is a defect dependent property and is not as sensitive to orientation and graphitic order. The presence of nanotubes and the development of graphite carbon in its vicinity (about 10 to 30 nm thick layer), most likely is a less defective structure than the surrounding glassy carbon. We think that these graphitic fibrils act as reinforcement, resulting in higher tensile strength fiber. For comparison, the tensile properties of the commercial carbon fibers are also listed in Table 7. As can be seen, the tensile modulus of the carbonized small diameter PAN/SWNT (99/1) fibers is higher than the PAN based T300 and IM8 fibers. Tensile strength and modulus of the experimental PAN/SWNT fibers can be further improved by process optimization.

In summary, gel spun PAN and PAN/SWNT composite fibers were stabilized and carbonized with varying stress. DSC showed significantly lower heat evolution in PAN/SWNT fibers under oxidative stabilization than in PAN, suggesting that the presence of SWNT hinders PAN reactivity. Infra-red spectroscopy showed that even after prolonged stabilization under stress, PAN/SWNT fiber contained more un-reacted nitrile than comparably stabilized PAN. The structure in stabilized PAN/SWNT appeared to be predominantly composed of conjugated nitrile, while in stabilized PAN it appeared to be composed of predominantly β-amino nitrile. Fibrillar structure was observed in the stabilized and carbonized PAN/SWNT, while the corresponding PAN fibers exhibited brittle fracture. Carbonized PAN in the immediate vicinity of SWNT is ductile while PAN carbonized farther away from carbon nanotubes or without carbon nanotubes is brittle. Carbonized PAN/SWNT fibers exhibit higher orientation, smaller graphite d-spacing and larger crystal size, than PAN carbonized under similar conditions. PAN/SWNT carbonized at 1100 ºC under stress shows the development of graphitic structure (as evidenced by Raman and high resolution transmission electron microscopy), while carbonized PAN showed only the presence of disordered carbon. Small diameter carbonized PAN/SWNT fibers containing 1 wt% SWNT exhibited 64% higher tensile strength and 49% higher tensile modulus than the corresponding carbonized PAN.

Tables 1. Properties and structural parameters of large diameter precursor gel spun PAN and PAN/SWNT (99/1) fibers used for carbon fiber processing.

|  | Control PAN | PAN/SWNT (99/1) |
|---|---|---|
| Draw ratio | 38 | |
| Linear density (tex) | 0.52 | 0.44 |
| Tensile modulus (N/tex) | $17.8 \pm 1.9$ | $22.5 \pm 1.9$ |
| Tensile strength (N/tex) | $0.72 \pm 0.12$ | $0.89 \pm 0.08$ |
| Strain to failure (%) | $7.9 \pm 1.2$ | $8.2 \pm 0.6$ |
| Crystallinity (%) | 65 | 68 |
| Crystallite size (nm) | 11.3 | 10.8 |
| $f_c$ | 0.916 | 0.927 |
| $f_{SWNT}$ | - | 0.904 |

Table 2. Heat of stabilization for large diameter PAN and PAN/SWNT fibers.

|  | $\Delta H_{stabilization}$ (kJ/g) | | |
|---|---|---|---|
|  | 1st run | 2nd run | 3rd run |
| Control PAN | 3.4 | 0.02 | - |
| PAN/SWNT (99.5/0.5) | 3.1 | 0.04 | 0.01 |
| PAN/SWNT (99/1) | 2.5 | 0.04 | 0.03 |

Table 3. Peak fitting results for FT-IR spectra of large diameter PAN and PAN/SWNT fibers stabilized under various conditions.

| | Precursor fiber | | HT-30 min at 285 °C (TGA) | | HT-furnace[2] (0.006 N/tex) | | HT-furnace[2] (0.025 N/tex) | |
|---|---|---|---|---|---|---|---|---|
| | PAN | PAN/ SWNT | PAN | PAN/ SWNT | PAN | PAN/ SWNT | PAN | PAN/ SWNT |
| Unreacted nitrile (%)[1] | 100 | 100 | 38.9 | 42.4 | 5.7 | 15.5 | 14.7 | 23.7 |
| Conjugated nitrile (%)[1] | - | - | 46.5 | 43.3 | 33.9 | 64.0 | 26.1 | 57.7 |
| β-amino nitrile (%)[1] | - | - | 14.6 | 15.3 | 60.4 | 20.5 | 59.2 | 18.6 |

[1] Area fraction by peak deconvolution.

[2] Stabilized in furnace at the indicated stress as per Figure 5.

Table 4 Structural parameters of large diameter stabilized PAN and PAN/SWNT fibers.

| Precursor | Applied stress (N/tex) | $f_c$ | $(28-26°)$ (nm) | $L_{(28-43°)}$ (nm) |
|---|---|---|---|---|
| Large diameter PAN | 0.025 | 0.421 | 1.2 | 1.8 |
| | 0.006 | 0.406 | 1.1 | 1.5 |
| Large diameter PAN/SWNT (99/1) | 0.025 | 0.432 | 1.2 | 2.3 |
| | 0.006 | 0.412 | 1.1 | 1.8 |

Table 5 Structural parameters of carbonized PAN and PAN/SWNT fibers.

| Precursor | Applied stress (N/tex) | $f_c$ | $Z^1$ (degree) | $d$-spacing$_{(002)}$ (nm) | $L_{(002)}$ (nm) | $L_{(10)}$ (nm) |
|---|---|---|---|---|---|---|
| Large diameter PAN | 0.025 | 0.763 | 33.9 | 0.349 | 1.2 | 1.7 |
| | 0.006 | 0.742 | 35.8 | 0.351 | 1.1 | 1.6 |
| Large diameter PAN/SWNT (99/1) | 0.025 | 0.798 | 31.2 | 0.344 | 1.3 | 1.8 |
| | 0.006 | 0.750 | 34.4 | 0.350 | 1.2 | 1.7 |
| Small diameter PAN/SWNT (99/1) | 0.025 | 0.795 | 31.4 | 0.345 | 1.3 | 2.1 |
| Commercial carbon fibers[3] | P-25 | - | 31.9 | 0.344 | 2.6 | 6 |
| | T-300 | - | 35.1 | 0.342 | 1.5 | 4 |
| | IM8 | - | - | 0.343 | 1.9 | 5 |

1 Full width at half maximum (FWHM) from azimuthal scans of (002) plane.

Table 6 Mechanical properties of stabilized large diameter PAN and PAN/SWNT fibers

| Precursor | Applied stress (N/tex) | Linear density (tex) | Tensile modulus (N/tex) | Tensile strength (N/tex) | Strain to failure (%) |
|---|---|---|---|---|---|
| Large diameter PAN | 0.025 | 0.58 | 12.7 ± 1.3 | 0.26 ± 0.05 | 4.7 ± 0.5 |
| | 0.006 | 0.77 | 8.7 ± 0.7 | 0.19 ± 0.03 | 5.2 ± 0.3 |
| Large diameter PAN/SWNT (99/1) | 0.025 | 0.41 | 16.0 ± 0.7 | 0.29 ± 0.02 | 4.5 ± 0.6 |
| | 0.006 | 0.64 | 11.3 ± 1.3 | 0.22 ± 0.03 | 4.6 ± 0.9 |

Table 7 Mechanical properties of carbonized PAN and PAN/SWNT fibers

| Precursor | Applied stress (N/tex) | Linear density (tex)* | Tensile modulus (N/tex)** | Tensile strength (N/tex)** | Strain to failure (%) |
|---|---|---|---|---|---|
| Large diameter PAN | 0.025 | 0.27 | 147 ± 13 | 1.1 ± 0.1 | 0.63 ± 0.08 |
| Large diameter PAN/SWNT (99.5/0.5) | | 0.25 | 184 ± 8 | 1.2 ± 0.1 | 0.65 ± 0.02 |
| Large diameter PAN/SWNT (99/1) | | 0.22 | 190 ± 9 | 1.4 ± 0.1 | 0.75 ± 0.04 |
| Small diameter PAN | | 0.064 | 168 ± 18 | 1.1 ± 0.2 | 0.68 ± 0.04 |
| Small diameter PAN/SWNT (99/1) | | 0.044 | 250 ± 27 | 1.8 ± 0.2 | 0.72 ± 0.05 |
| Commercial carbon fibers[4] | P-25 | 0.179*** | 84 | 0.7 | 0.9 |
| | T-300 | 0.067*** | 129 | 1.8 | 1.5 |
| | IM8 | 0.037*** | 172 | 2.9 | 1.9 |

* tex is the mass in grams of 1000 m length of fiber.

** N/tex is same as GPa divided by density in $g/cm^3$.

*** Linear density of the commercial carbon fibers was calculated based on the diameter and density data reported by the manufacturer.
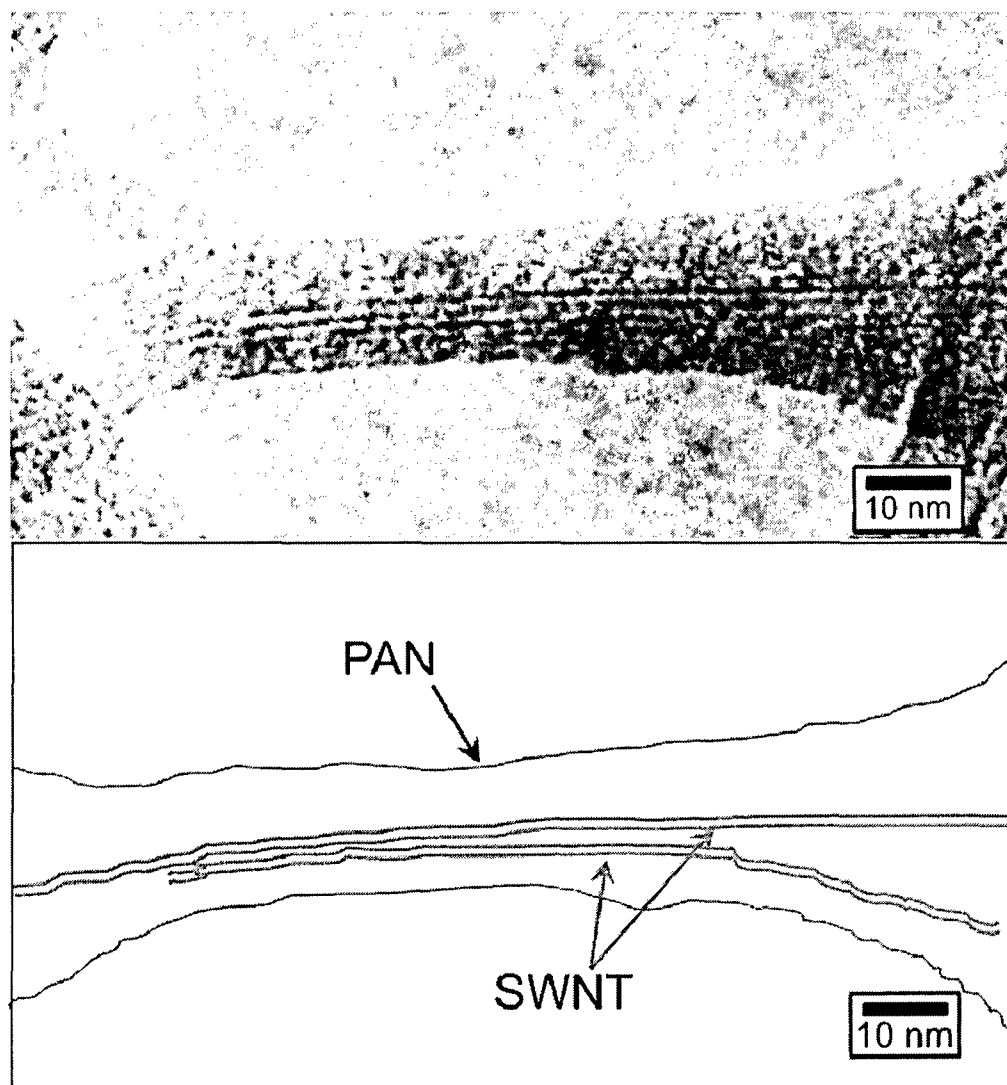
Figure 1. The schematic and HR-TEM image of the precursor PAN/SWNT (99/1) fiber. TEM samplewas prepared by boiling the precursor fiber in DMFand by placing a drop of the dispersion on the lacey carbon grid.
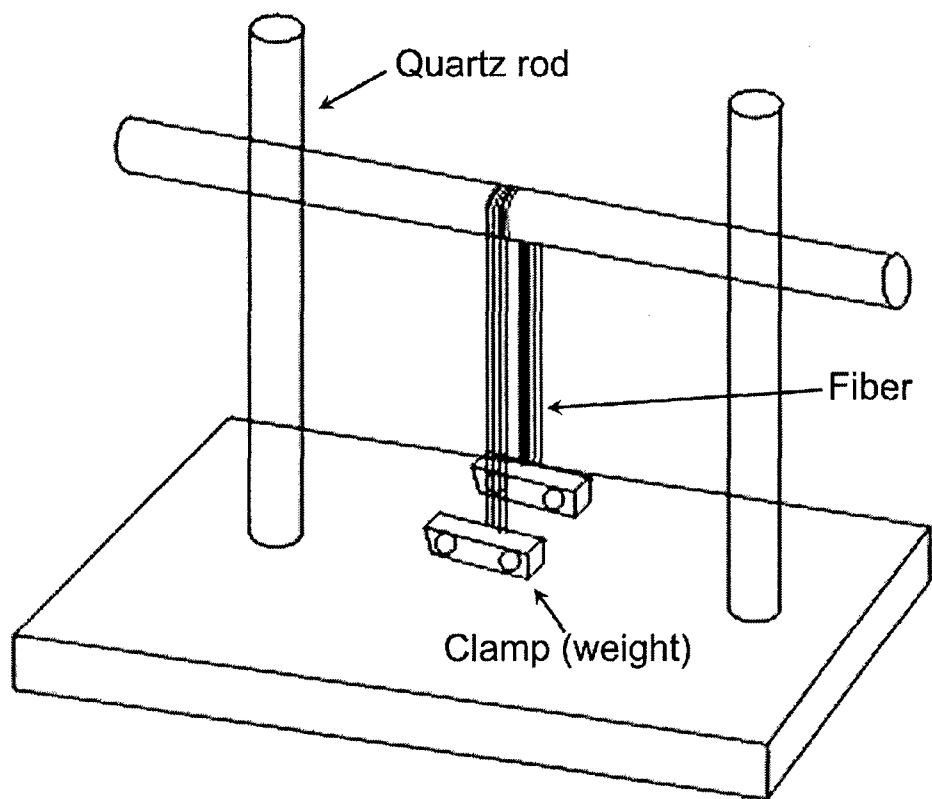
Figure 2. The schematic of the experimental setup for stabilization and carbonization.
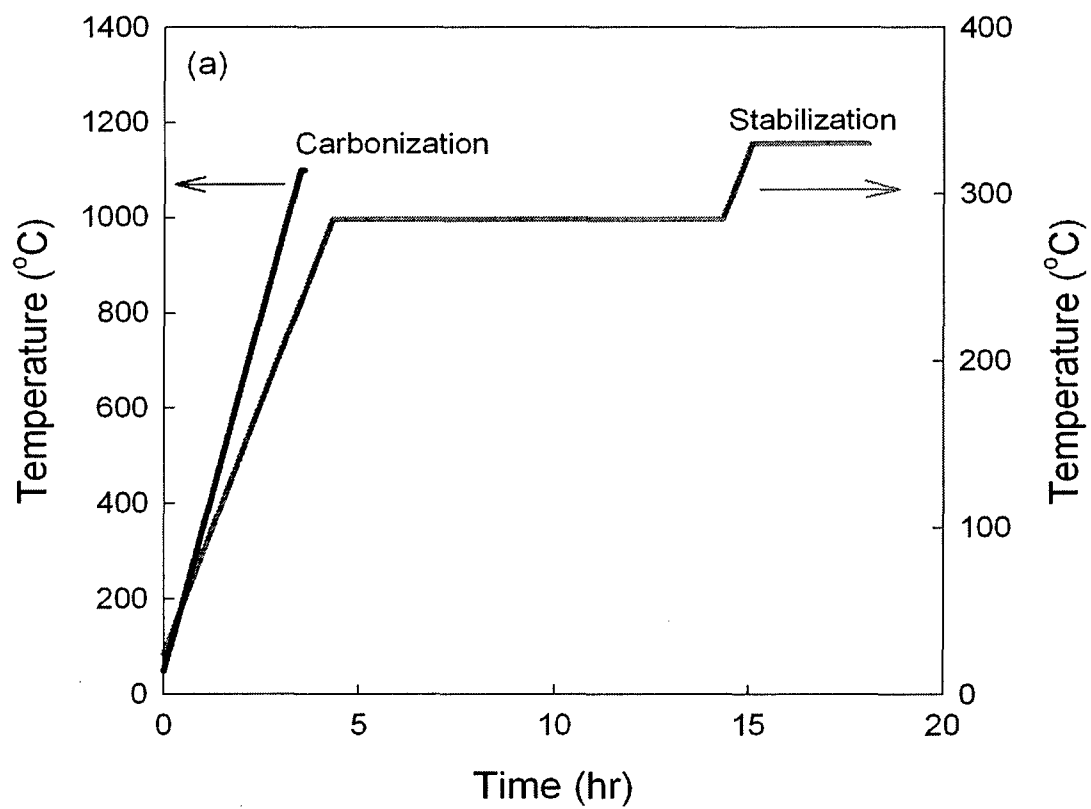
Figure 3. Temperature profiles for stabilization and carbonization: (a) large diameter fiber and (b) small diameter fiber.
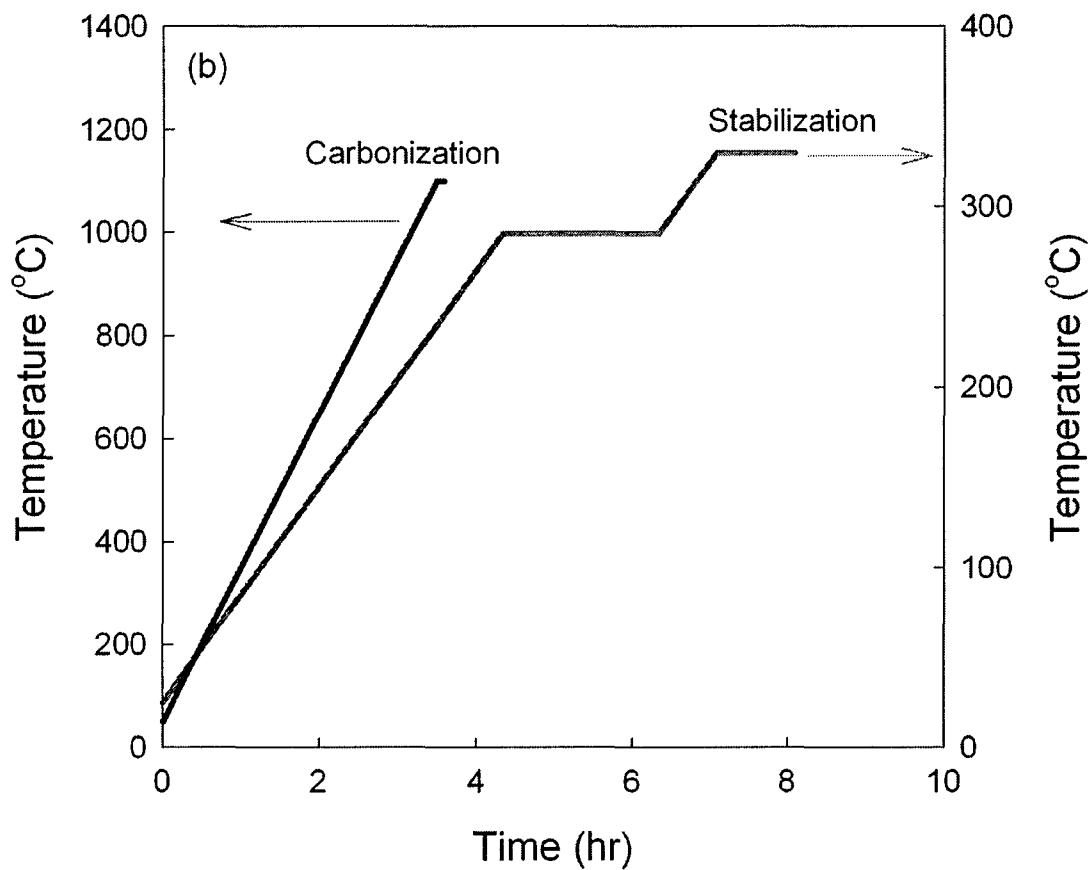
Figure 3. Temperature profiles for stabilization and carbonization: (a) large diameter fiber and (b) small diameter fiber.
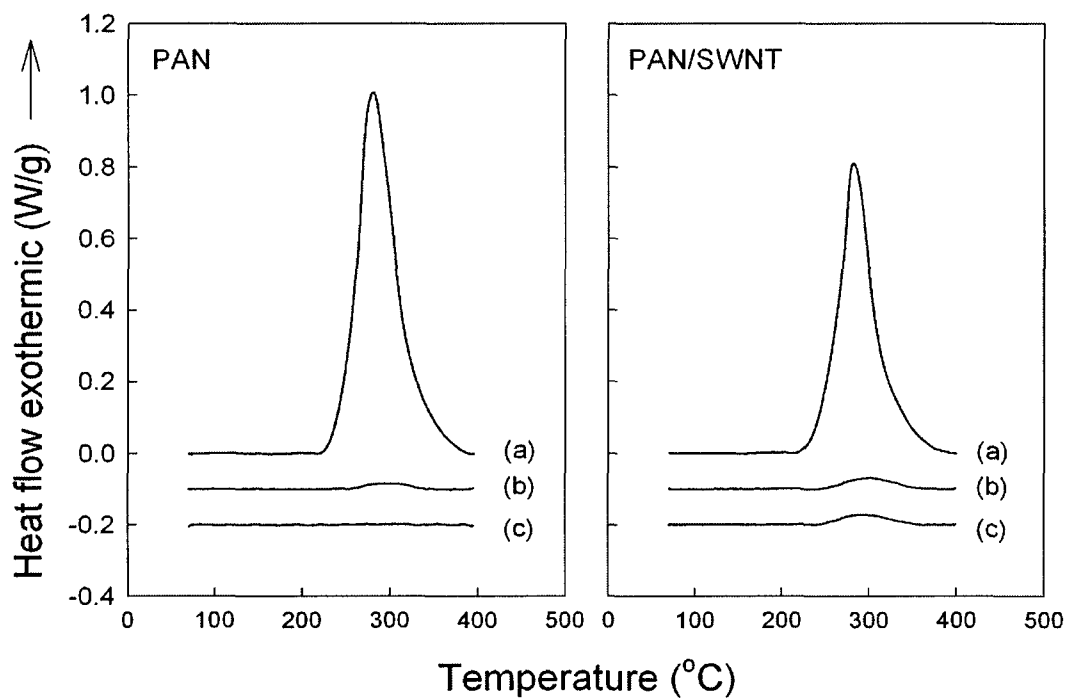
Figure 4. DSC thermograms of large diameter gel spun PAN and PAN/SWNT (99/1) fibers: (a) 1st, (b) 2nd, and (c) 3rd heating cycle at 1 $^{o}$C/min.
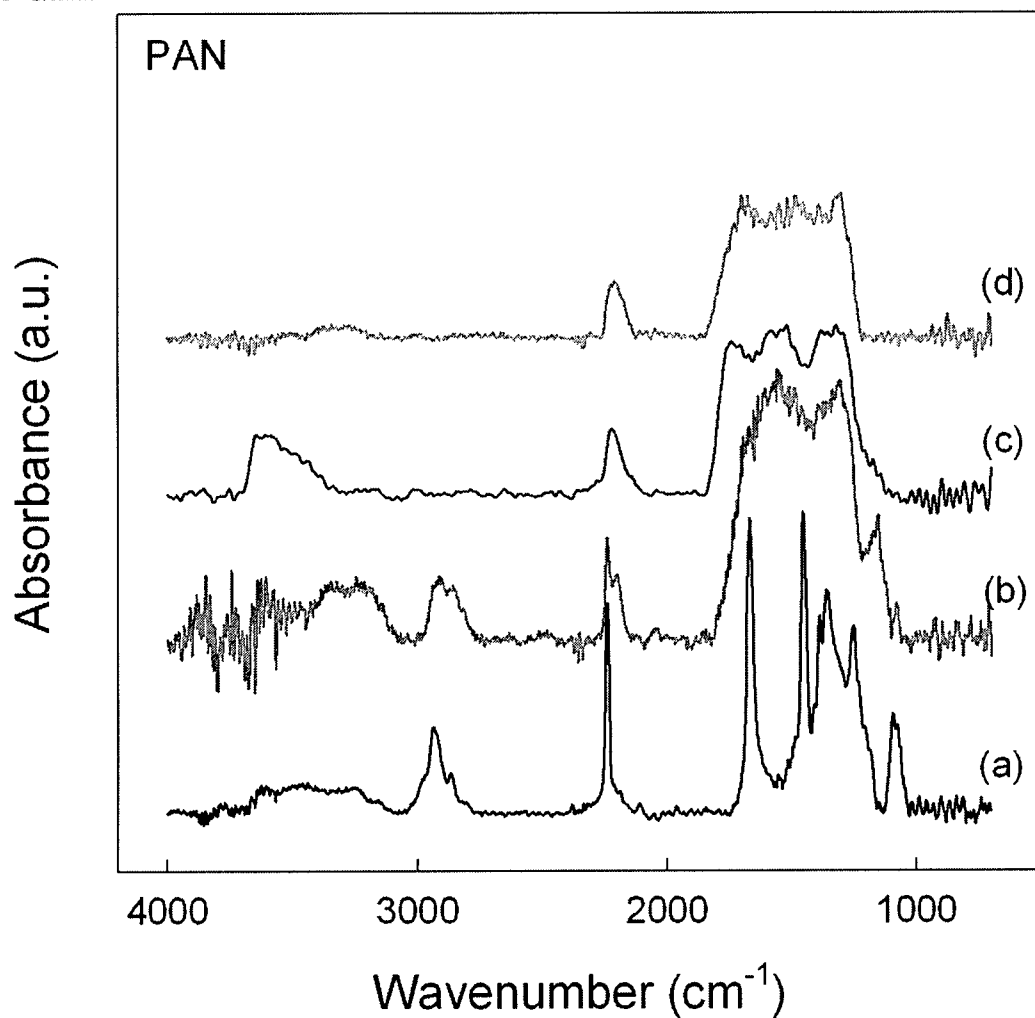


Figure 5. FT-IR spectra for large diameter PAN and PAN/SWNT (99/1) fibers: (a) precursor fibers, (b) stabilized in TGA at 285 $^{o}$C for 30 min in air, (c) stabilized in furnace at 0.006 N/tex stress, and (d) stabilized in furnace at 0.025 N/tex stress in air.
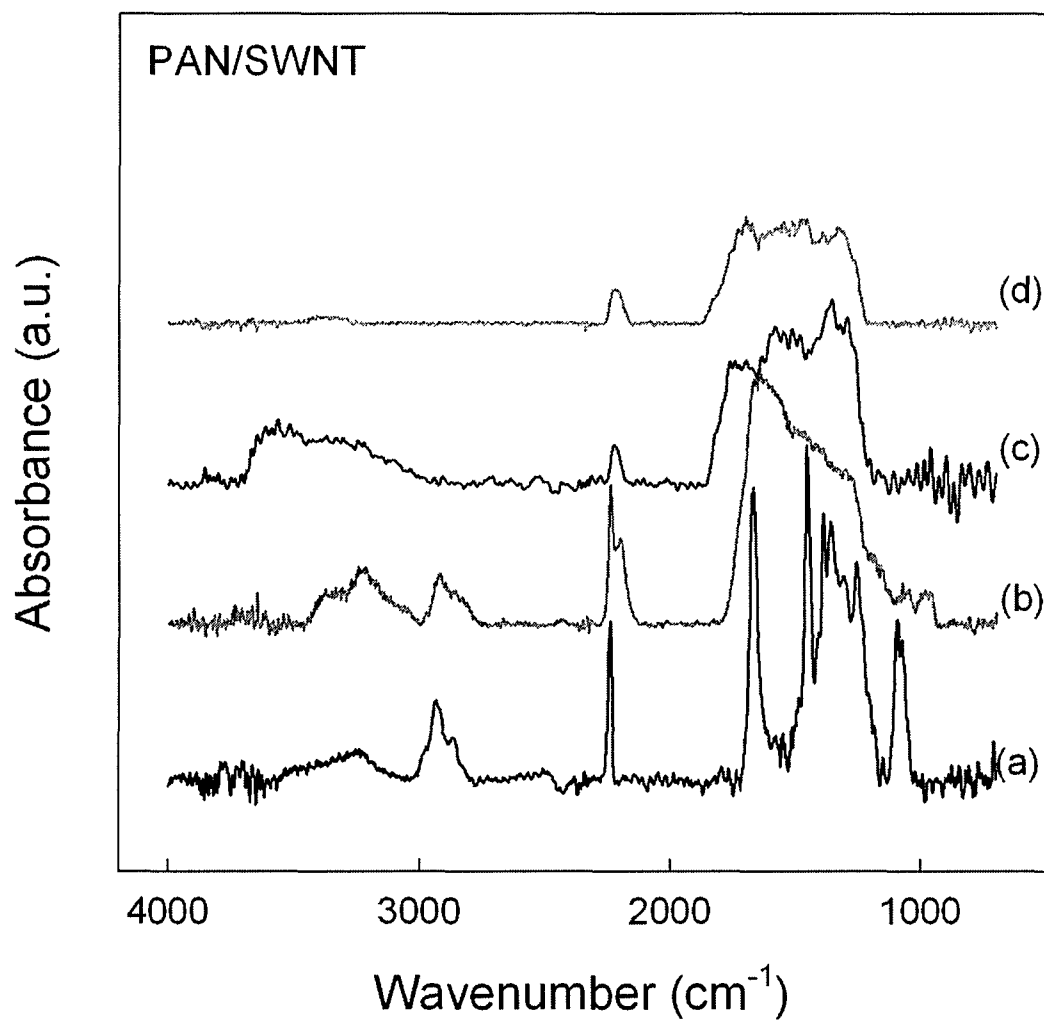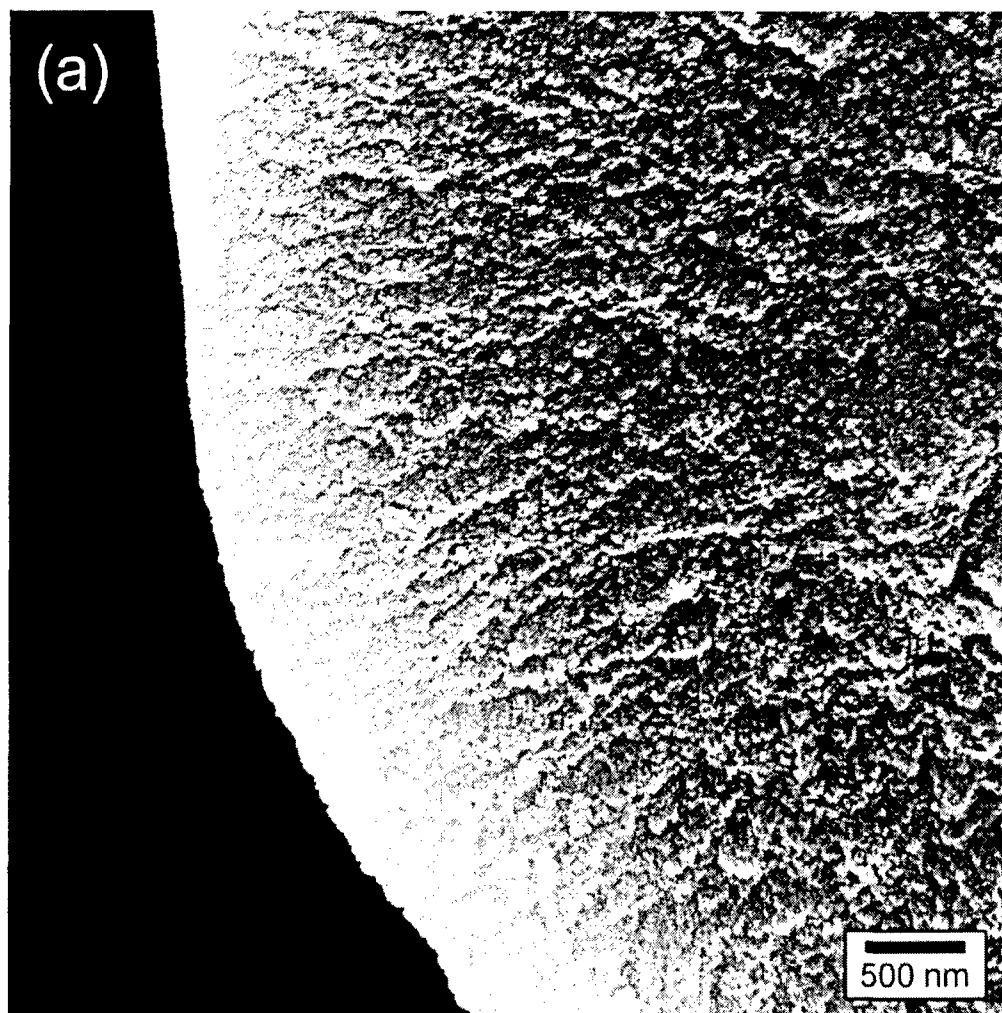
Figure 5. FT-IR spectra for large diameter PAN and PAN/SWNT (99/1) fibers: (a) precursor fibers, (b) stabilized in TGA at 285 °C for 30 min in air, (c) stabilized in furnace at 0.006 N/tex stress, and (d) stabilized in furnace at 0.025 N/tex stress in air.
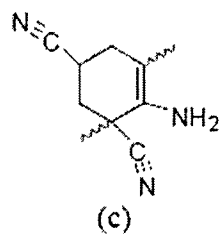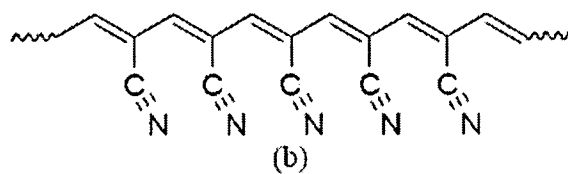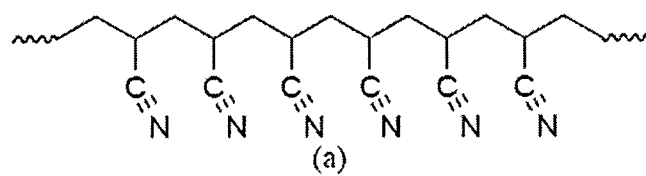
Figure 6. Chemical structure of various nitrile groups: (a) unreacted, (b) conjugated, and (c) β-amino nitrile.
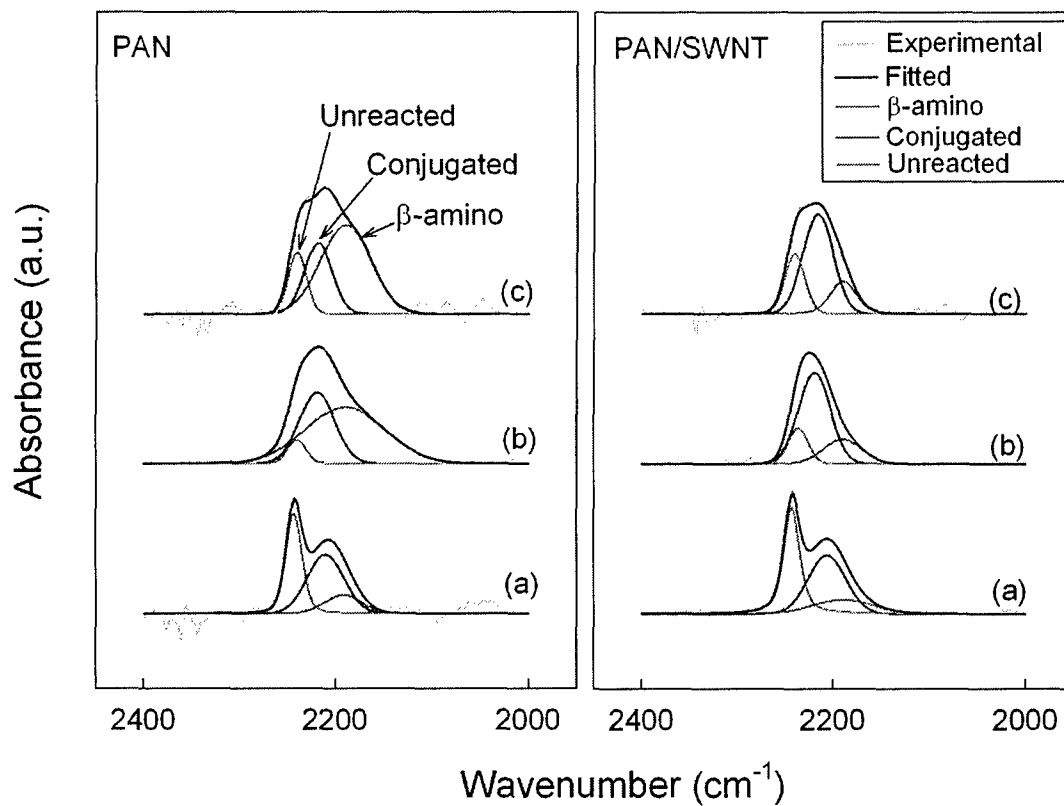
Figure 7. Nitirle band peak fitting results for large diameter PAN and PAN/SWNT (99/1) fibers: (a) stabilized in TGA at 285 °C for 30 min in air, (b) stabilized in furnace at 0.006 N/tex stress, and (c) stabilized in furnace at 0.025 N/tex in air.
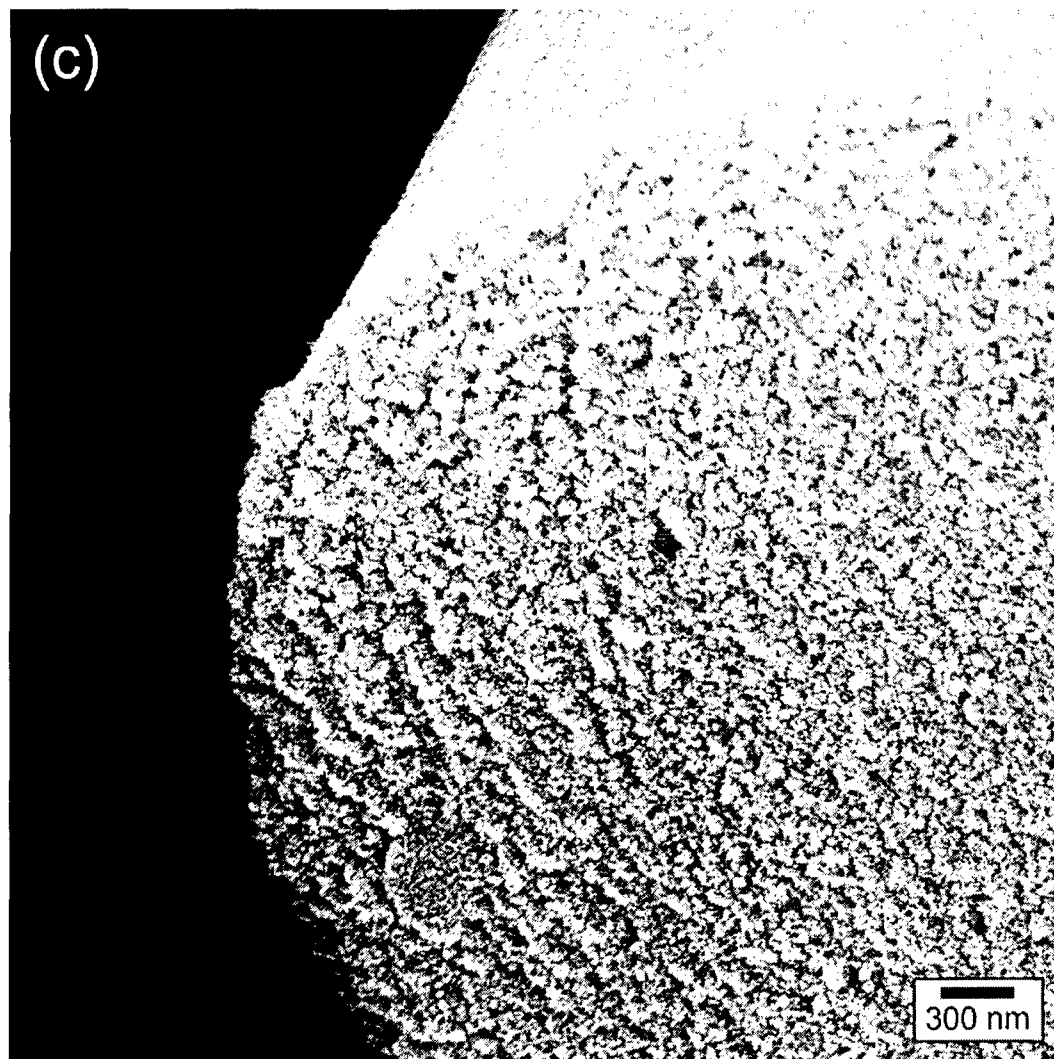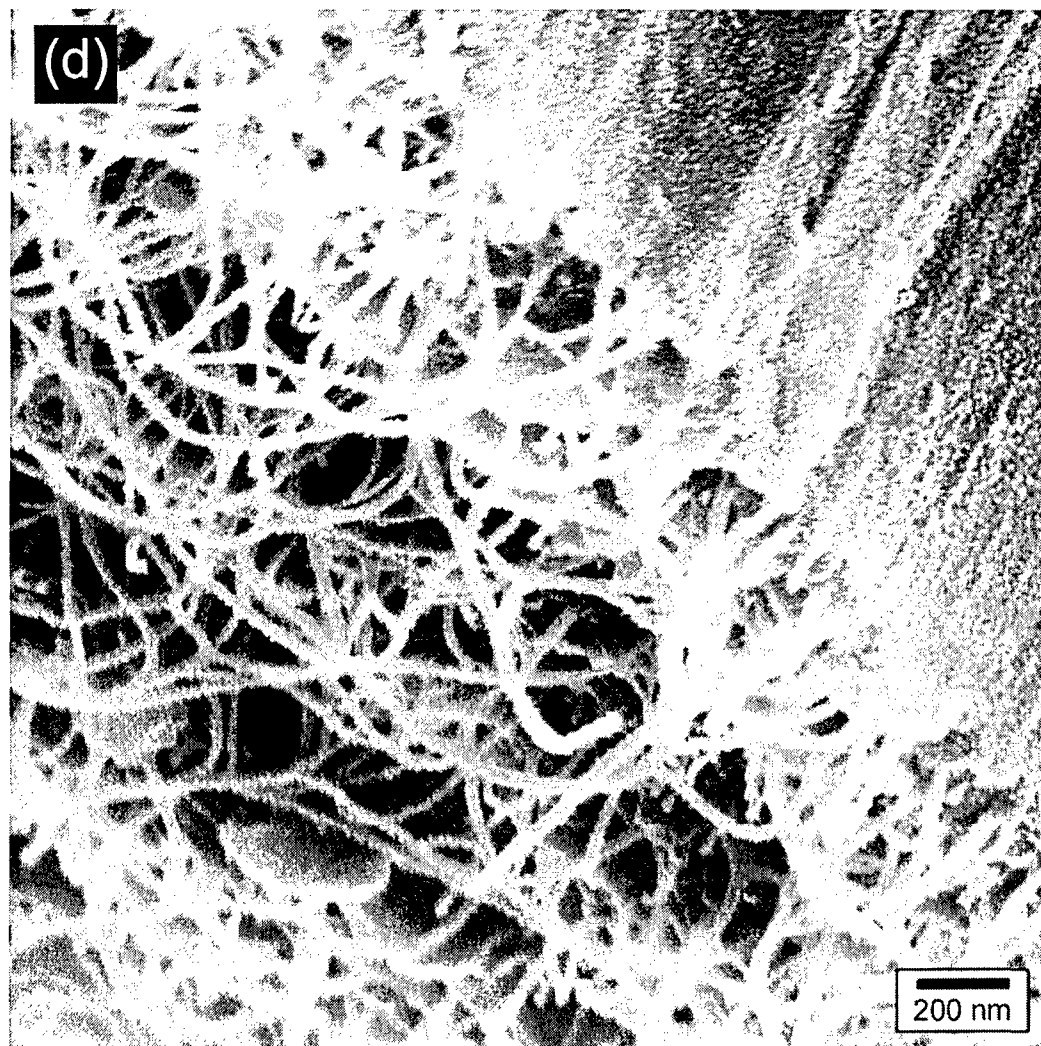
Figure 8. SEM micrographs for the large diameter (a) stabilized PAN and (b) stabilized PAN/SWNT (99/1), and the (c) carbonized PAN and (d) carbonized PAN/SWNT (99/1) fibers.
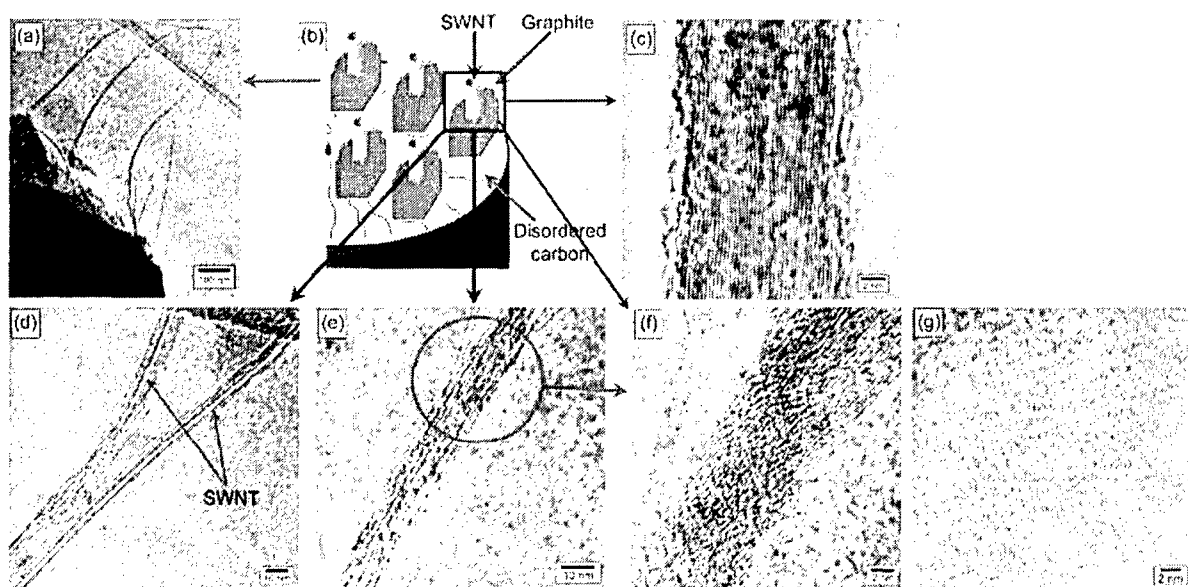
Figure 8. SEM micrographs for the large diameter (a) stabilized PAN and (b) stabilized PAN/SWNT (99/1), and the (c) carbonized PAN and (d) carbonized PAN/SWNT (99/1) fibers.

Figure 8. SEM micrographs for the large diameter (a) stabilized PAN and (b) stabilized PAN/SWNT (99/1), and the (c) carbonized PAN and (d) carbonized PAN/SWNT (99/1) fibers.

Figure 8. SEM micrographs for the large diameter (a) stabilized PAN and (b) stabilized PAN/SWNT (99/1), and the (c) carbonized PAN and (d) carbonized PAN/SWNT (99/1) fibers.

Figure 9. HR-TEM images and schematic (a to f) of carbonized PAN/SWNT (99/1) fiber. For comparison, HR-TEM image of carbonized PAN is also given (g).
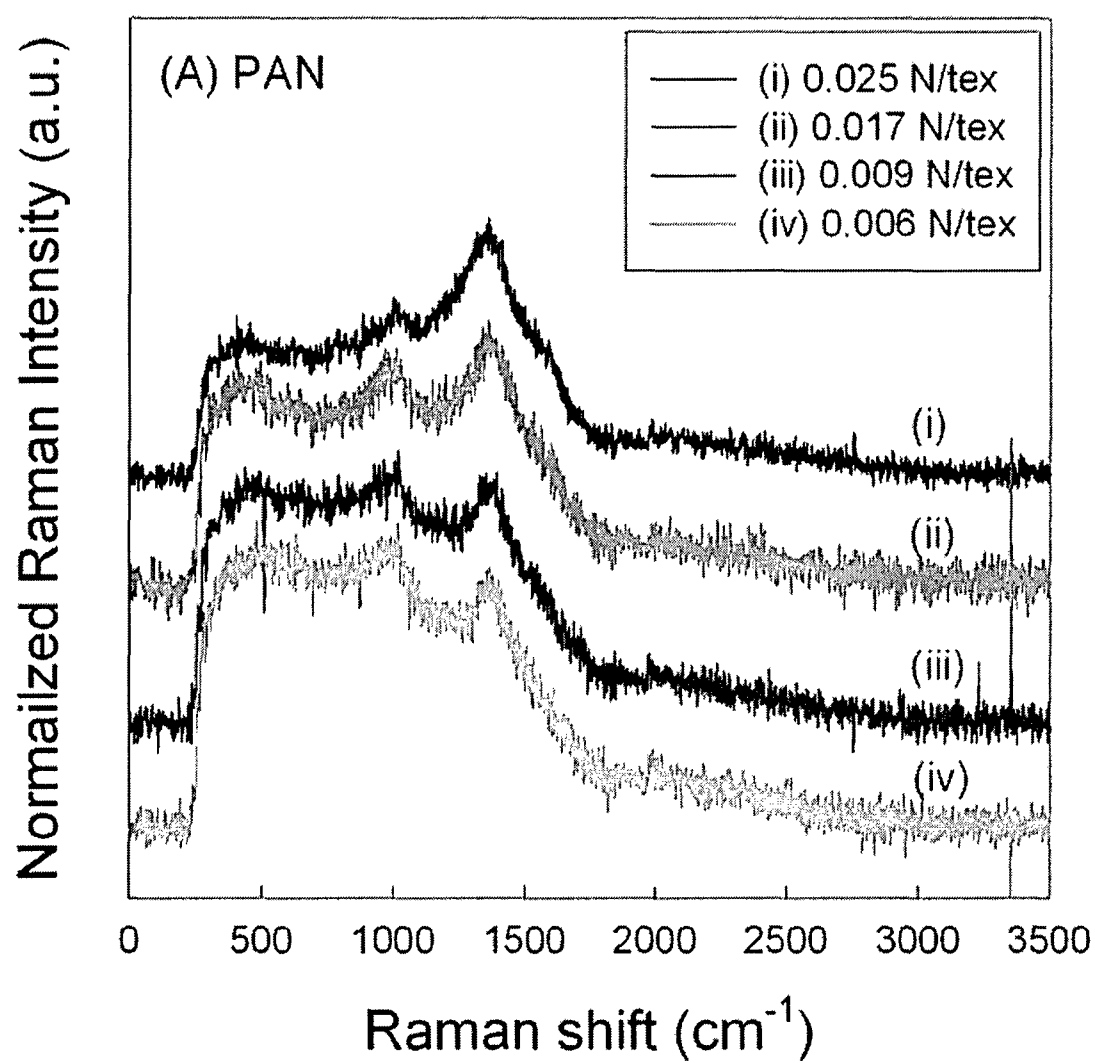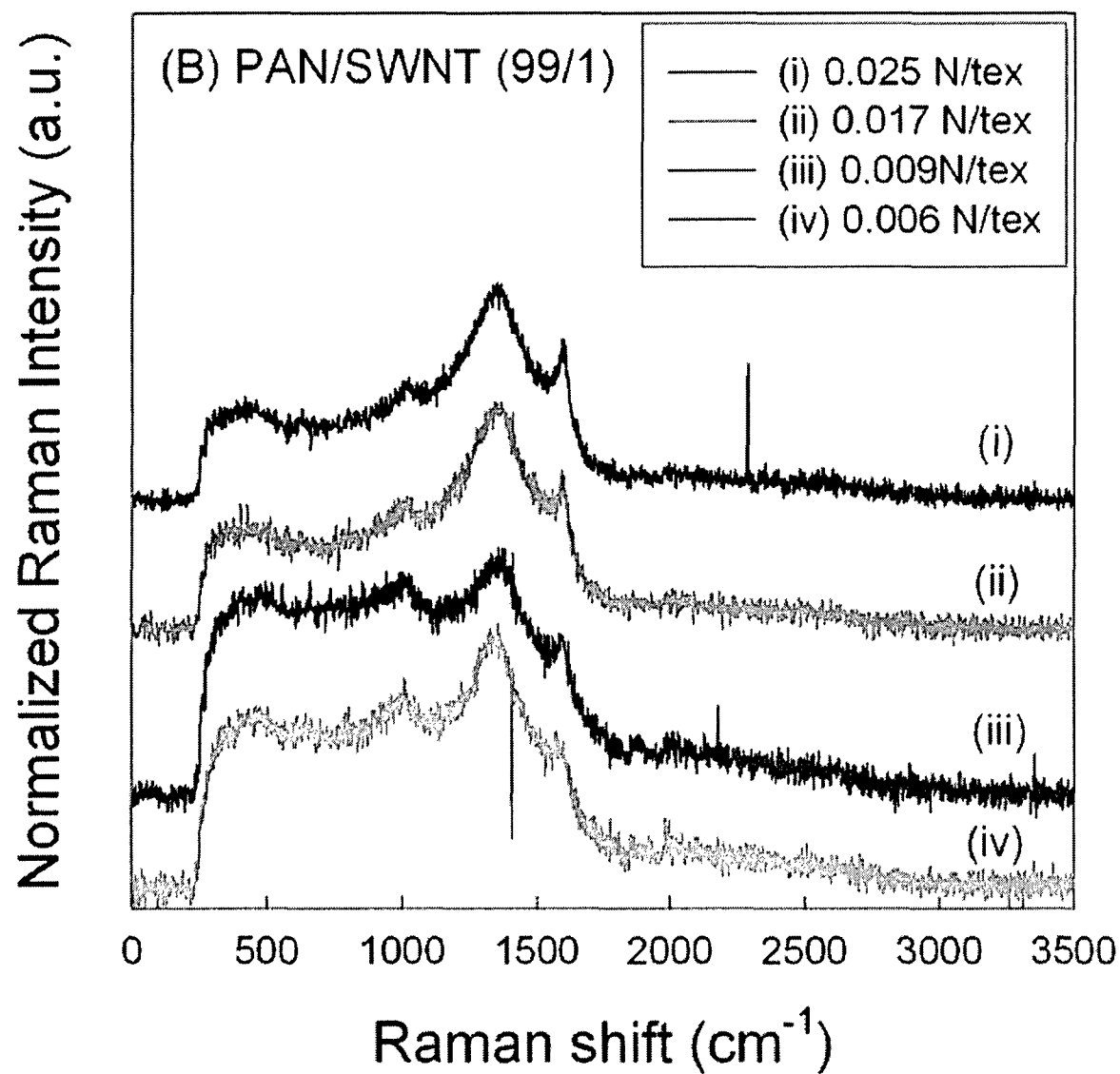
Figure 10. Raman spectra for the carbonized (A) PAN and (B) PAN/SWNT (99/1) fibers as a function of applied stress during stabilization and carbonization.

Figure 10. Raman spectra for the carbonized (A) PAN and (B) PAN/SWNT (99/1) fibers as a function of applied stress during stabilization and carbonization.
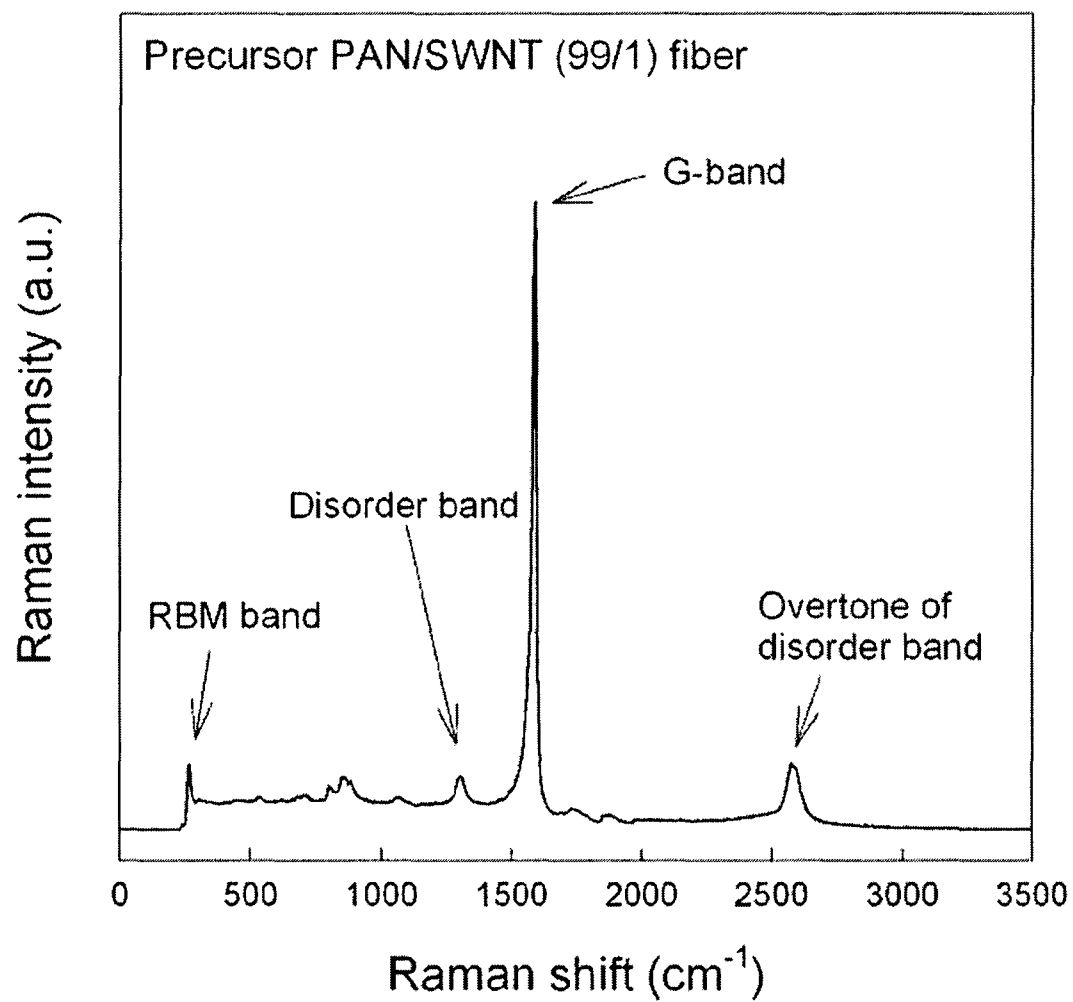
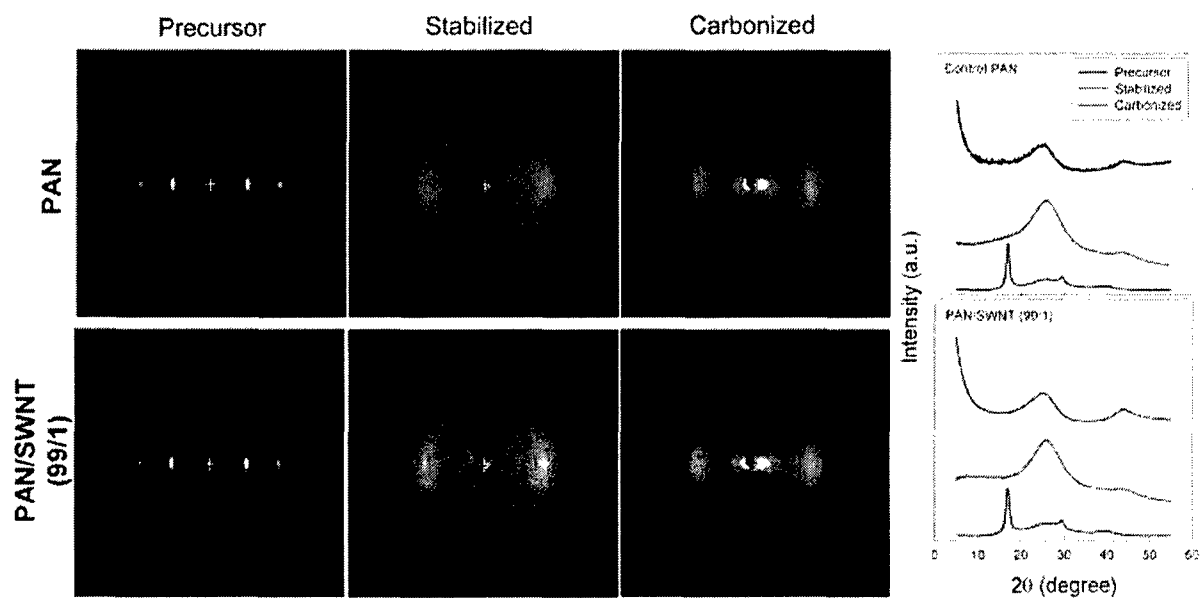Figure 11. Raman spectrum of the precursor gel spun PAN/SWNT (99/1) fiber.

Figure 12. WAXD patterns and integrated scans of the precursor, stabilized, and carbonized PAN and PAN/SWNT (99/1) fibers.
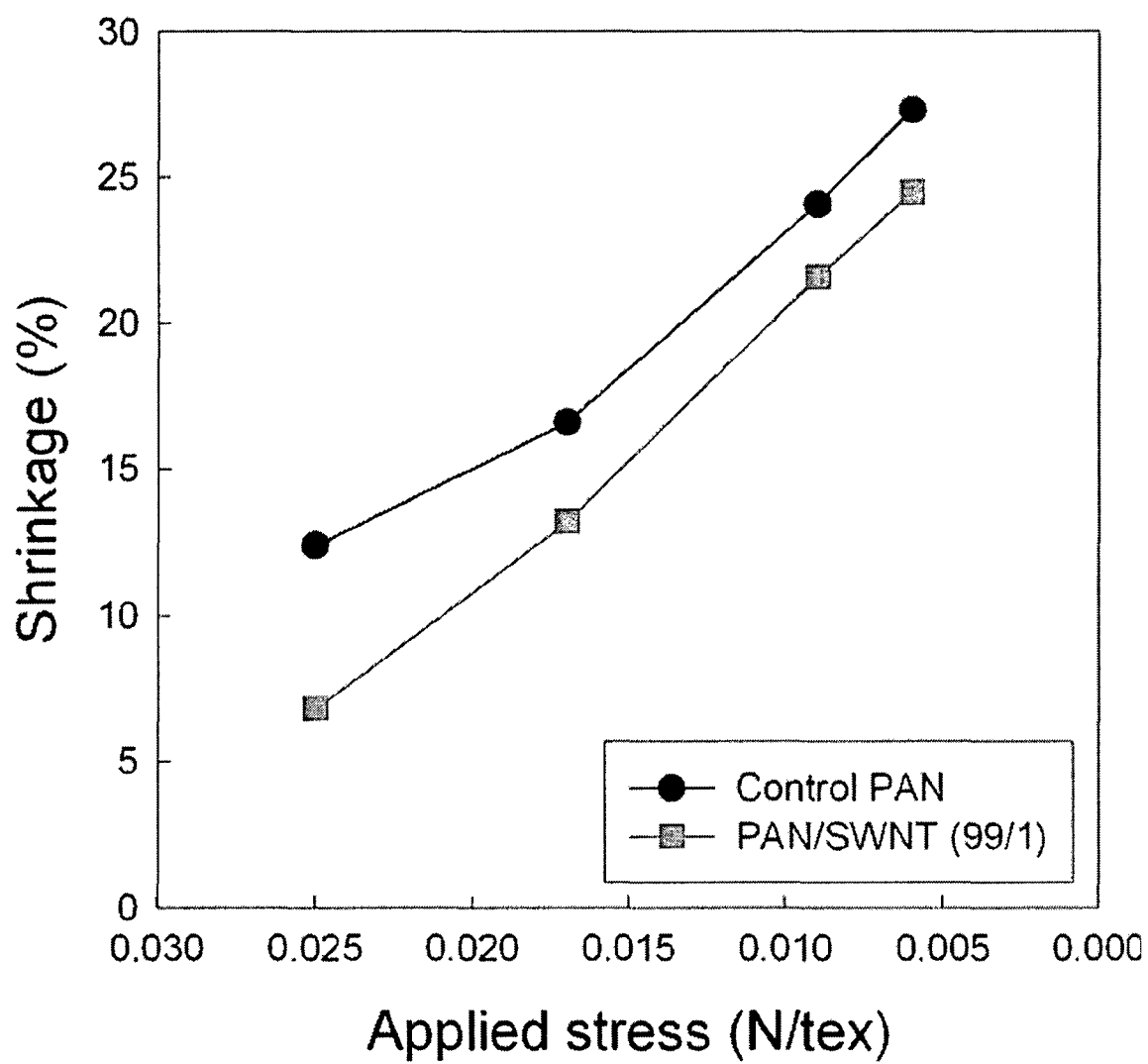
Figure 13. Fiber shrinkage behavior after stabilization as a function of applied stress.

# References

[1]     Bahl OP, Shen Z, Lavin JG, Ross RA. In Manufacture of Carbon Fibers. Marcel Dekker. New York, 1998; p 1.

[2]     Donnet J-B, Bansal RC. In Carbon Fibers. Marcel Dekker. New York, 1984.

[3]     Kumar S, Anderson DP, Crasto AS. Journal of Materials Science 1993;28:423-39.

[4]     Minus ML, Kumar S. JOM 2005;57:52-8.

[5]     Peebles LH. In Carbon Fibers - Formation, Structure, and Properties. CRC Press, Inc. Boca Raton, 1995.

[6]     Peebles LH, Yanovsky YG, Sirota AG, Bogdanov VV, Levit PM. In Mechanical Properties of Carbon Fibers. Marcel Dekker. New York, 1998; p 311.

[7]     Chae HG, Sreekumar TV, Uchida T, Kumar S. Polymer 2005;46:10925-35.

[8]     Sreekumar TV, Liu T, Min BG, Go H, Kumar S, Hauge RH, Smalley RE. Advanced Materials 2004;16:1583-.

[9]     Chae HG, Minus ML, Kumar S. Polymer 2006;47:3494-504.

[10] Koganemaru A, Bin Y, Agari Y, Matsuo M. Advanced Functional Materials 2004;14:842-50.

[11] Zhu D, Koganemaru A, Xu CY, Shen QD, Li SL, Matsuo M. Journal of Applied Polymer Science 2003;87:2063-73.

[12] Zhu D, Xu CY, Nakura N, Matsuo M. Carbon 2002;40:363-73.

[13]    Min BG, Sreekumar TV, Uchida T, Kumar S. Carbon 2005;43:599-604.

[14] Sivy GT, Gordon B, Coleman MM. Carbon 1983;21:573-8.

[15] Fochler HS, Mooney JR, Ball LE, Boyer RD, Grasselli JG. Spectrochimica Acta Part a-Molecular and Biomolecular Spectroscopy 1985;41:271-8.

[16]    Shimada I, Takahagi T, Fukuhara M, Morita K, Ishitani A. Journal of Polymer Science Part a-Polymer Chemistry 1986;24:1989-95.

[17]    Usami T, Itoh T, Ohtani H, Tsuge S. Macromolecules 1990;23:2460-5.

[18]    Zhu Y, Wilding MA, Mukhopadhyay SK. Journal of Materials Science 1996;31:3831-7.

[19] Devasia R, Reghunadhan CP, Sivadasan NP, Katherine BK, Ninan KN. Journal of Applied Polymer Science 2003;88:915-20.

[20]    Samuels RJ. In Structured Polymer Properties. John Wiley & Sons. New York, 1974.

[21] Cullity BD, Stock SR. In Elements of X-ray Diffraction. Prentice Hall. Upper Saddle River, 2001.

[22] Ge JJ, Hou HQ, Li Q, Graham MJ, Greiner A, Reneker DH, Harris FW, Cheng SZD. Journal of the American Chemical Society 2004;126:15754-61.

[23] Guo H, Sreekumar TV, Liu T, Minus M, Kumar S. Polymer 2005;46:3001-5.

[24]    Ko F, Gogotsi Y, Ali A, Naguib N, Ye HH, Yang GL, Li C, Willis P. Advanced Materials 2003;15:1161-5.

[25]    Uchida T, Kumar S. Journal of Applied Polymer Science 2005;98:985-9.

[26]    Weisenberger MC, Grulke EA, Jacques D, Rantell T, Andrews R. Journal of Nanoscience and Nanotechnology 2003;3:535-9.

[27]    Ye HH, Lam H, Titchenal N, Gogotsi Y, Ko F. Applied Physics Letters 2004;85:1775-7.

[28] Gallaher KL, Lukco D, Grasselli JG. Canadian Journal of Chemistry-Revue Canadienne De Chimie 1985;63:1960-6.

[29]    Coleman MM, Petcavich RJ. Journal of Polymer Science Part B-Polymer Physics